Preonics (foundation of optics)

In this section we will show that optics, or the behaviour of light, is governed the laws of momentum.

In fact, if QGD is correct, the same equations may be used to describe the dynamics of interacting objects however small or large they may be.

Reflection of Light

The third law of momentum we derived from the axiom set of QGD says that momentum can change only by discrete amounts. That is: $\left\|\Delta\vec{F}_a\right\| = xm_a$ where $x \in N$ and a can be any particle or material structure.

When the trajectory of a photon γ and that of an electron e^- intersect, the same mechanism we described earlier applies. That is, γ will emit $preons^{(+)}$ in the direction of e^- such that $\vec{P}_\gamma^{\,\to e^-} = \vec{P}_\gamma \cos\theta_1$ where $\vec{P}_\gamma^{\,\to e^-}$ is the momentum vector component of γ in direction of e^-, $\vec{P}_\gamma$ is the momentum vector of γ and θ_1 is the angle between $\vec{P}_\gamma$ and the line connecting the centers of γ and e^-. Similarly, $\vec{P}_{e^-}^{\,\to\gamma} = \vec{P}_{e^-}\cos\theta_2$.

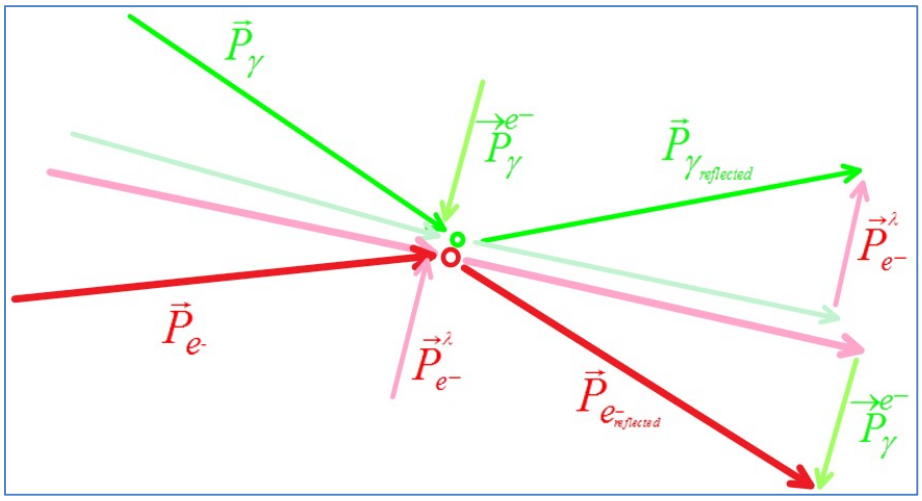

$Preons^{(+)}$ emitted by the electron will be absorbed by the photon so that $\vec{P}_{\gamma_{reflected}} = \vec{P}_\gamma - \vec{P}_\gamma^{\,\to e^-} + \vec{P}_{e^-}^{\,\to\gamma}$ and $\vec{P}_{e^-_{reflected}} = \vec{P}_{e^-} - \vec{P}_{e^-}^{\,\to\gamma} + \vec{P}_\gamma^{\,\to e^-}$ as a result, γ will and e^- be reflected from each other as shown in the figure above. This mechanism describes and explains the Compton scattering when $\vec{P}_\gamma^{\,\to e^-} > \vec{P}_{e^-}^{\,\to\gamma}$ and inverse Compton scattering when $\vec{P}_\gamma^{\,\to e^-} < \vec{P}_{e^-}^{\,\to\gamma}$.

The Electromagnetic Effects of Attraction of Repulsion

The preonic field is composed of free $preons^{(+)}$ uniformly distributed in quantum-geometrical space. Free $preons^{(+)}$ interact with particles or structures matter in accordance to the laws of momentum which as we have seen govern preonics of which is a generalization of optics. When interacting with a particle or structure, $preons^{(+)}$ are absorbed and emitted following the structure of the particle or structure. When the components of a particles or structures are random, the absorbed and reflected $preons^{(+)}$ are also random so that the momentum of the neighbouring preonic field is equal to zero. That is: $\vec{P}_{\Theta} = \sum_{i=1}^{m_{\Theta}} \vec{c}_i = \vec{0}$.

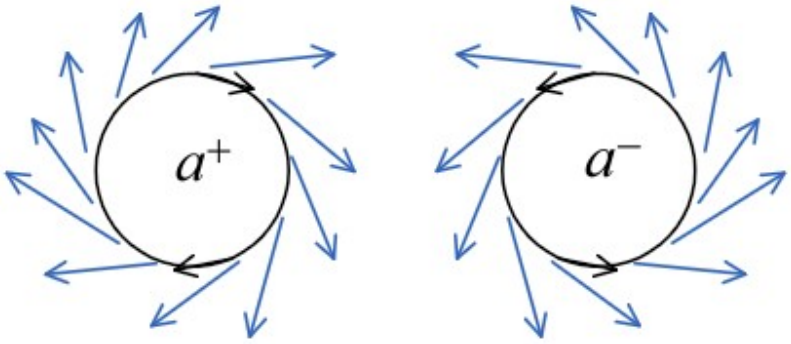

However when the components of the particle or structure (electrons for example) are aligned in which case the absorbed and reflected $preons^{(+)}$ will consequently be aligned. Such particles or structures which components motions are aligned are called charged. The interactions between the preonic field and a charged particle or structure cause the polarization the preonic field which we call the magnetic field. From the discussion about optical reflection we know that the direction of the reflection will depend on the direction of the particles the $preons^{(+)}$ will interact with. The figure above is a diagram that shows the dependency of the reflection of $preons^{(+)}$ on the orientation of a particle or structure. The black vectors represent the direction of the components of the particles or structures a^+ and a^-, and the blue vectors represent the polarization of the preonic field in the regions neighbouring them.

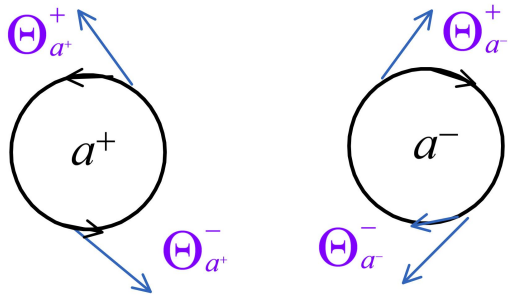

When two charged particles or structures come into proximity, they each interact with regions of each other's polarized preonic field. The figure on the left shows how we will represent and label charged particles or structures and the interacting regions of the polarized preonic field.

Compton Scattering and the Repulsion and Attraction of Charged Particles.

We have shown in the section on reflection of light that when applying the laws of momentum to the interaction between photons and atomic electron that the Compton scattering occurs when $\overrightarrow{P}_{\gamma}^{e^-} > \overrightarrow{P}_{e^-}^{\gamma}$ and the inverse Compton scattering when $\overrightarrow{P}_{\gamma}^{e^-} < \overrightarrow{P}_{e^-}^{\gamma}$ where γ is the incident photon and $\overrightarrow{P}_{\gamma}^{e^-}$ and $\overrightarrow{P}_{e^-}^{\gamma}$ are respectively the momentum of the $preons^{(+)}$ emitted by the electron and the momentum imparted by the photon with which it interacts. Conservation of momentum requires that the momentum of the electron must change by a vector of equal magnitude but inverse direction of the sum of $\overrightarrow{P}_{\gamma}^{e^-}$ and $\overrightarrow{P}_{e^-}^{\gamma}$. That is, $\Delta\vec{P}_{e^-} = -\left(\overrightarrow{P}_{\gamma}^{e^-} + \overrightarrow{P}_{e^-}^{\gamma}\right)$. This implies that if $\overrightarrow{P}_{\gamma}^{e^-} > \overrightarrow{P}_{e^-}^{\gamma}$ then the momentum vector of the electron will increase in the direction opposite of the point of interaction by $\Delta\vec{P}_{e^-}$. Inversely, if $\overrightarrow{P}_{\gamma}^{e^-} < \overrightarrow{P}_{e^-}^{\gamma}$ then the electron's momentum vector will increase towards the point of interaction by $\Delta\vec{P}_{e^-}$. Whether we have a Compton or reverse Compton scattering depends on the relative direction of the photon and electron (or particle or structure). That is, based on the laws of momentum, if the photon and electron at the point of interaction move directly towards each other, then $\overrightarrow{P}_{\gamma}^{e^-} > \overrightarrow{P}_{e^-}^{\gamma}$ and if their trajectories intersect tangentially, then $\overrightarrow{P}_{\gamma}^{e^-} < \overrightarrow{P}_{e^-}^{\gamma}$. The Compton scattering and its inverse are special cases of preonic interactions which can explain the effects of repulsion and attraction of charged particles.

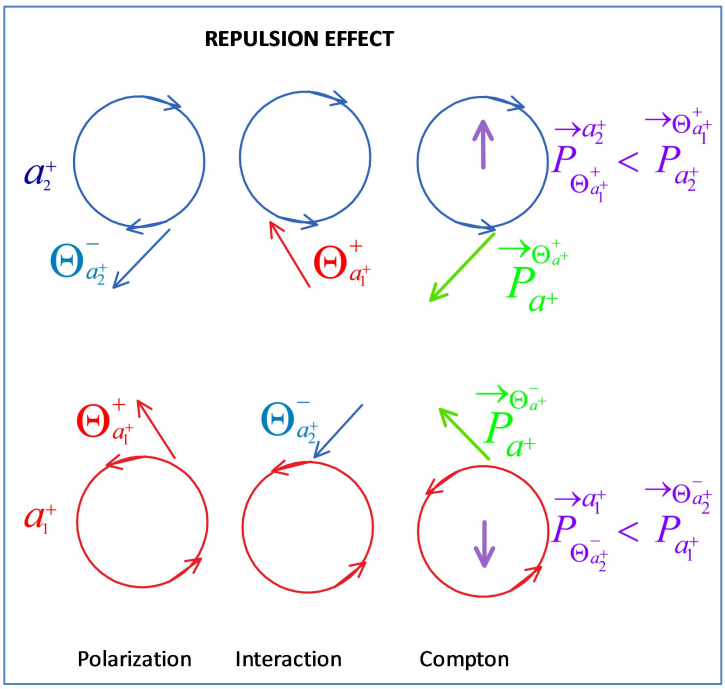

The figure on the left illustrates the interaction between two oppositely charged particles (a^+ and a^-) . The circular vectors represent the angular momentum of the particles and the blue and red vectors correspond to the direction of the polarization preonic field respectively. Since the polarization of $\Theta^+_{a_1^+}$ is opposite to orientation of a_2^+ then $\overrightarrow{P}^{\rightarrow a_2^+}_{\Theta^+_{a_1^+}} < P^{\rightarrow \Theta^+_{a_1^+}}_{a_2^+}$ and $\Delta\vec{P}_{a_2^+}$ will point away from $\Theta^+_{a_1^+}$, thus a_2^+ will move away from a_1^+. Similarly, the polarization of $\Theta^-_{a_2^+}$ is opposite the orientation of a_1^+ so that $\overrightarrow{P}^{\rightarrow a_1^+}_{\Theta^-_{a_2^+}} < P^{\rightarrow \Theta^-_{a_2^+}}_{a_1^+}$, consequently a_1^+ will move away from a_2^+. This explains the effect of repulsion between two similarly charged particles (and structures).

In the figure on the right, we have to particles of opposing charges. Here since the polarization of the region $\Theta^+_{a^+}$ is opposite to the orientation of a^- and the region $\Theta^-_{a^-}$ is polarized in opposite the orientation of a^+ then $\overrightarrow{P}^{\rightarrow a^-}_{\Theta^+_{a^+}} > \overrightarrow{P}^{\rightarrow \Theta^+_{a^+}}_{a^-}$ and $\overrightarrow{P}^{\rightarrow a^+}_{\Theta^-_{a^-}} > \overrightarrow{P}^{\rightarrow \Theta^-_{a^-}}_{a^+}$ and as a result $\Delta\vec{P}_{a^+}$ will point to a^- and $\Delta\vec{P}_{a^-}$ will point to a^+. Therefore a^+ and a^- will move towards each other and appear to

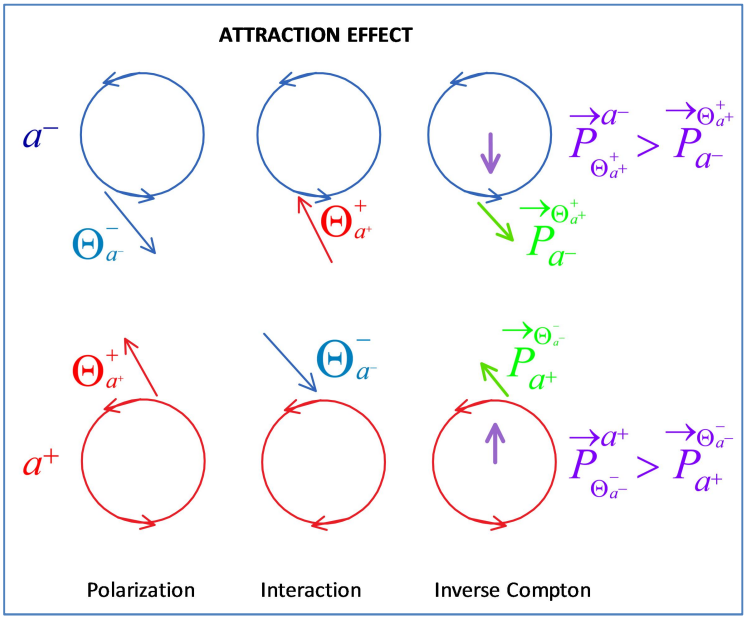

be attracting.

As we shown, the observed repulsion between like charges and attraction between opposite charges does not result from repulsion and attraction between the particles themselves but from their interactions between the preonic regions polarized by other particles.

Also, since the polarized $preons^{(+)}$ are emitted radially from a charged particle or structure, the intensity or momentum of the polarized region follows the inverse square law. In fact the inverse square law of the momentum of a magnetic field is a consequence of QGD's preonics.

Interaction Between Large Charged Structures and the Preonic Field

Large structures composed that have aligned charged particles behave in the way we have described in the preceding section. The main difference is that the effect of a large number of aligned charged particles creates more intense polarization over a much larger region of the preonic field.

The intensity of the magnetic field at a distance r from a charged structure is $\vec{P}_{\Theta_r} \propto \frac{\Theta_{dens} S_a a_{dens}}{r^2}$ where Θ_{dens} is the density of the preonic field or $\Theta_{dens} = \frac{m_\Theta}{vol_\Theta}$, S_a is the surface of the interacting particle or structure and a_{dens} is the density of aligned electrons on the surface of a .

Note: In a following section, we will discuss how the dynamics of atomic electrons follow from QGD's laws of momentum.

Refraction of Light

Changes in momentum of an electron are discrete increments proportional to its mass, that is, $\left\|\Delta\vec{P}_{e^-}\right\| = m_{e^-}$.

Now consider a photon γ_0 interacting with an atomic electron with $xm_{e^-} \le \left\|\vec{P}_{\gamma}^{\to e^-}\right\| < (x+1)m_{e^-}$

where $\vec{P}_{\gamma}^{\to e^-}$ is the momentum vector of the photon emitted by γ_0 in direction of e^- as a component of the interaction as we explained earlier, and $\vec{P}_{e^-}^{\to \gamma} \ll \vec{P}_{\gamma}^{\to e^-}$.

To be consistent with the laws of momentum transfer, $\Delta\vec{P}_{e^-} = m_{e^-}\dfrac{\vec{P}_{\gamma_0}^{\to e^-}}{\left\|\vec{P}_{\gamma_0}^{\to e^-}\right\|}$ so upon absorption of the $preons^{(+)}$ emitted by γ_0 the electron must emit a photon λ_1 such that $\vec{P}_{\gamma_1} = \vec{P}_{\gamma_0} - \Delta\vec{P}_{e^-}$ (see figure below). This is the basic mechanism of refraction.

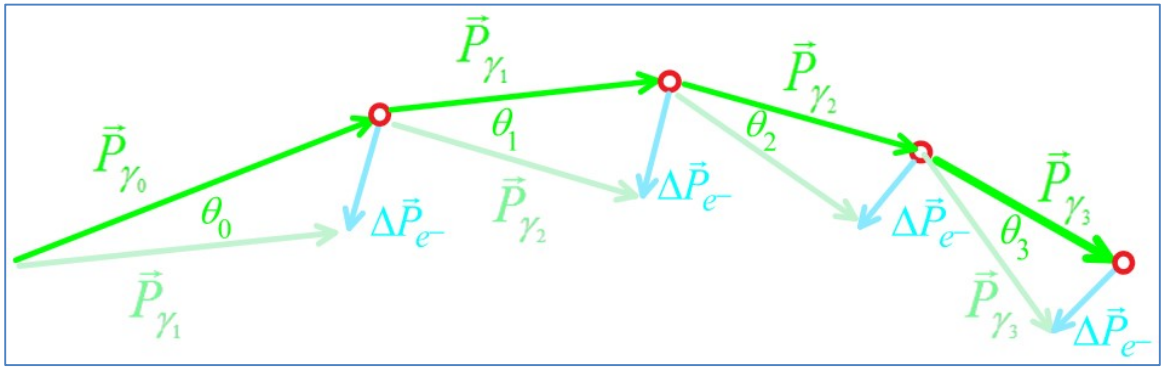

From the equation, we see that θ_0, the angle between γ_0 and γ_1 (angle of refraction), is inversely proportional to $\vec{P}_{\gamma_0}$. That is, the greater the momentum (which corresponds to higher energy or higher frequency in accepted physics), then the greater the refraction for a single interaction. But the refraction of light, by a prism for example, is the result of a series of interactions.

That is: since $xm_{e^-} \le \left\|\vec{P}_{\gamma_0}^{\to e^-}\right\| < (x+1)m_{e^-}$, then for $i \ge x+1$ we have $\left\|\vec{P}_{\gamma_i}^{\to e^-}\right\| < m_{e^-}$ and $\vec{P}_{\gamma_i} = \vec{P}_{\gamma_{i+1}}$ and as a consequence $\theta_i = 0$. So there is no refraction for photons once

$\left\| \vec{P}_{\gamma_i}^{e^-} \right\| < m_{e^-}$. The point at which a photon achieves maximum refraction is directly proportional to its momentum and this produces the colour separation by prism.

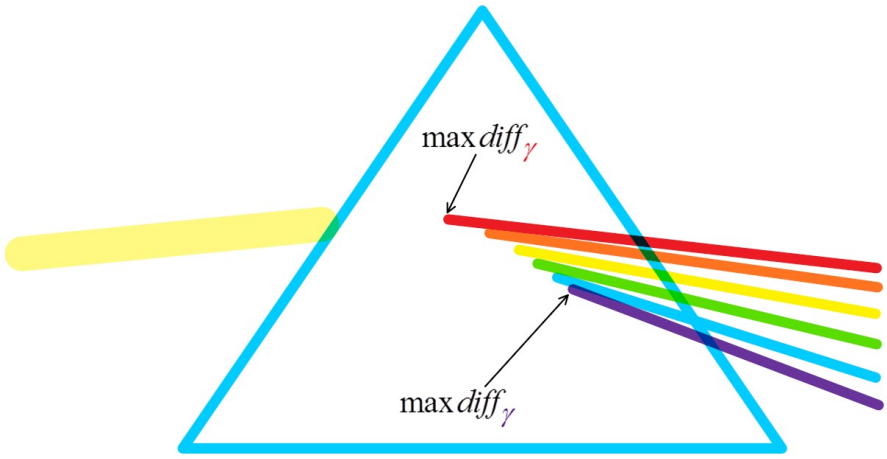

Note that the shape of the prism is ideal as it allows for photons of different momentums to achieve maximum diffraction.

If the number of refractive interactions is lower than what is necessary for photons to achieve maximum refraction, then the colours will be separated due to reflection and as we have seen, the angle of reflection is smaller the higher the momentum is. That explains why refraction using a grid is smaller for photons with higher momentums than photons with lower momentums.

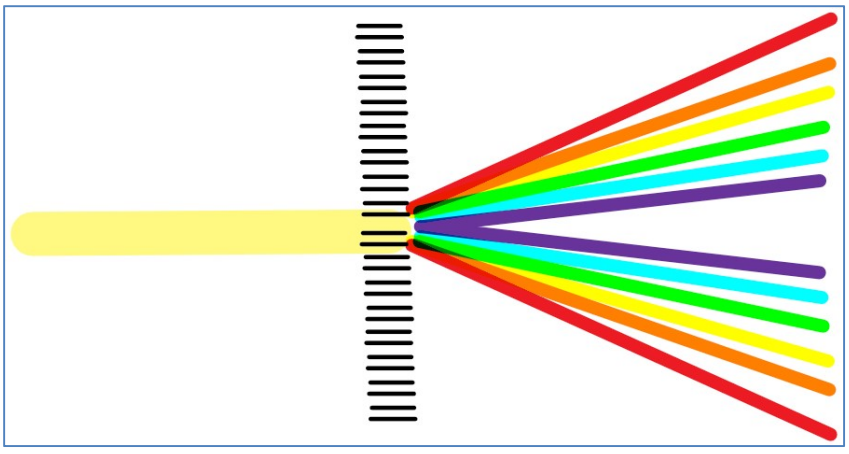

Diffraction of Light

Diffraction is a simple consequence of reflection, that is, the interaction between light and matter and not, as thought, between light waves.

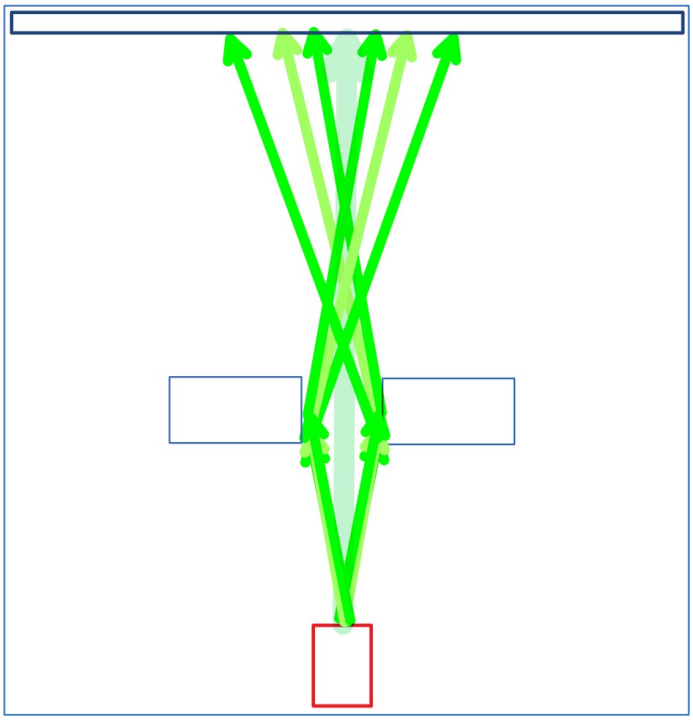

The light bands of diffraction patterns correspond to the allowed changes in momentum of particles or structures and the dark bands correspond to the forbidden changes in momentum.

The bands will appear if there is one source of light and the photons composing the light are have similar momentum. Applying our understanding of reflection of light, we find that the reflection angle of a photon depends not only on its angle of incidence but also on its momentum. The smaller the angle, the smaller will be the momentum from the electron it interacts with and the smaller will the momentum and angle of reflection of the reflected photon. The angle of reflection of a photon is close to but not equal to the incident angle.

In a strict description the reflection, we must also consider that that only certain changes in momentum are allowed as per our description of momentum and momentum transfer we saw here. So if $\vec{P}^{\to\gamma}_{e^-}$ is the momentum emitted by the electron in direction of the photon γ with which it interacts and if $xm_\gamma < \vec{P}^{\to\gamma}_{e^-} < (x+1)m_\gamma$, then $\Delta\vec{P}_\gamma = xm_\gamma$ so that all photons within a range of incident angle will be reflected at the same exact angle, but that none will be reflected at angles in the between the exact angle of reflection (this is only true of course for photons of the same momentum). The result will be as described in the figure above.

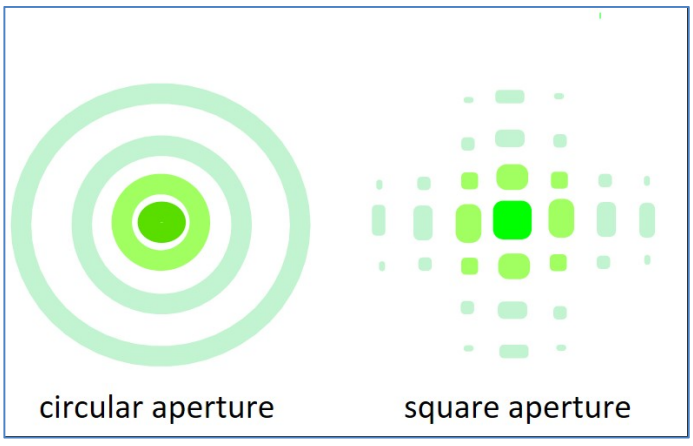

The width between the bands but is proportional to difference between the allowable momentums changes they correspond to given a slit of the same depth and width.

As for the number of dark fringes, we will show in the next section that it is proportional to the number of allowed changes in

momentum within the angles of diffraction permitted by the aperture. That is: $n_{fringes} = 2\left|\frac{\left\|\vec{P}_\gamma \cos\theta_{\max}\right\|}{m_{e^-}}\right|$ where $\theta_{\max}$ is half the aperture angle and $n_{fringes}$ is the number dark fringes on the x or y axis.

As for the pattern of diffraction, it will depend on the shape of the aperture. Applying the equations we have introduced we can predict the patterns generated by a group of photons.

Fringe Patterns from Double-slit Experiments

Following the failure of classical physics theories to explain the interference patterns observed in double slit experiments and other light diffraction experiments and because of the similarities

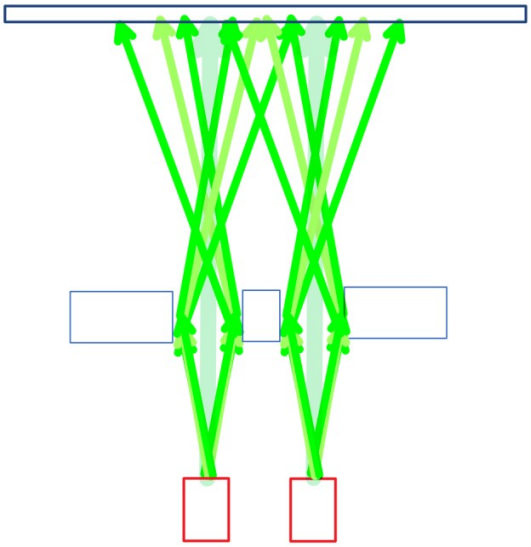

between these patterns and the interference patterns generated by waves at the surface of a liquid, physicists deduced that light was behaving as a wave which led to the so-called wave-particle duality of light. Since the particle model could explain phenomena such as the photoelectric effect and since the wave model of light described the interference patterns of light, it made sense to deduce that light had to corpuscular or wave-like depending on the experiment performed on it. But what experiments actually showed is that neither accepted models of light could explain both behaviours and emphasized the need for a new theory.

The patterns generated in double-slit experiment are thought to be the results of interferences between light waves, but they can be better understood in terms of the reflection and absorption patterns of photons through a mechanism consistent with the laws governing optics (or more generally, preonics) .

Though we describe the double-slit experiments that use photons, the same explanation applies for electrons or any other particle.

Single Slit Experiment

We will first describe single slit experiments.

The momentum vector components that can be imparted to an electron is given by $\left\|\vec{P}_\gamma \cos\theta\right\|$ where θ is the angle between the $\vec{P}_\gamma$ and $\vec{P}_{e^-}$, but from the laws of momentum we know that

the momentum imparted by γ must be such that $\left\|\Delta\vec{P}_{e^-}\right\| = \alpha m_{e^-}$ and we have $\alpha = \left|\frac{\left\|\vec{P}_\gamma \cos\theta\right\|}{m_{e^-}}\right|$.

So the momentum that can be imparted to an electron by a photon is $\left\|\Delta\vec{P}_{e^-}\right\| = \left|\frac{\left\|\vec{P}_\gamma \cos\theta\right\|}{m_{e^-}}\right| m_{e^-}$.

We see that when $\vec{P}_\gamma$ is perpendicular to $\vec{P}_{e^-}$, $\left\|\vec{P}_\gamma \cos\theta\right\| = 0$ so that the photon is reflected back. As we move away from that angle towards, the photon will be absorbed when θ is such that $\left\|\vec{P}_\gamma \cos\theta\right\| = m_{e^-}$. This will show as a dark fringe on the screen which width depends on the width of the slit and the distance the slit and the screen.

The number of absorption fringes will be equal to $n_{fringes} = 2\left|\frac{\left\|\vec{P}_\gamma \cos\theta_{\max}\right\|}{m_{e^-}}\right|$.

Double-Slit Experiments

When there are two slits, two or more photons from different angles can simultaneously interact with an electron. In the case of two photons, they will be absorbed if $\left\|\vec{P}_{\gamma_1} \cos\theta_1 + \vec{P}_{\gamma_2} \cos\theta_2\right\| = \alpha m_{e^-}$. If this condition is not met, then both photons γ_1 and γ_2 will be reflected.

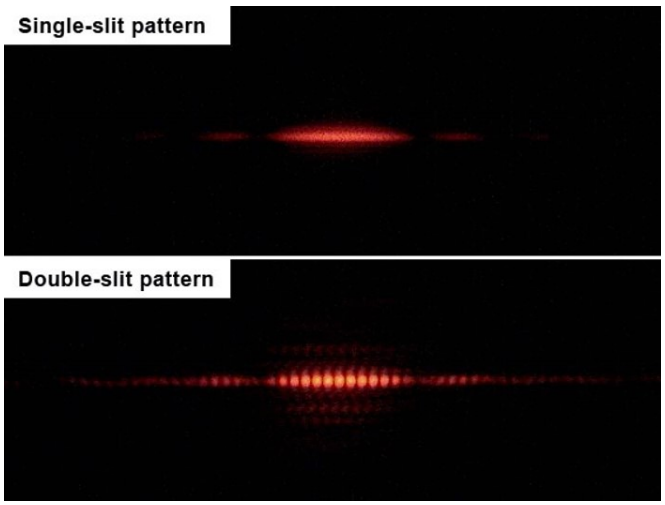

At the centre of the screen (which is the point on the screen that is at equal distance from both slits), $\left\|\vec{P}_{\gamma_1} \cos\theta_1 + \vec{P}_{\gamma_2} \cos\theta_2\right\| = 0$ and the photons will be reflected. But away from the centre, we there will be angles θ_1 and θ_2 such that $\left\|\vec{P}_{\gamma_1} \cos\theta_1 + \vec{P}_{\gamma_2} \cos\theta_2\right\| = \alpha m_{e^-}$ creating dark fringes which width depend on the width of the slits and the distances from each other and the screen.

As for the number of dark fringes (absorption fringes), it is a function of the angular ranges of photons from the two slits.

From the mathematical description we find that the momentum of the photons will affect the distances between the fringes. Everything else being equal, the greater the momentum of photons, the closer adjacent absorption fringes will be as shown in the picture below which compares the patterns emerging from photons of three momentums (energies).

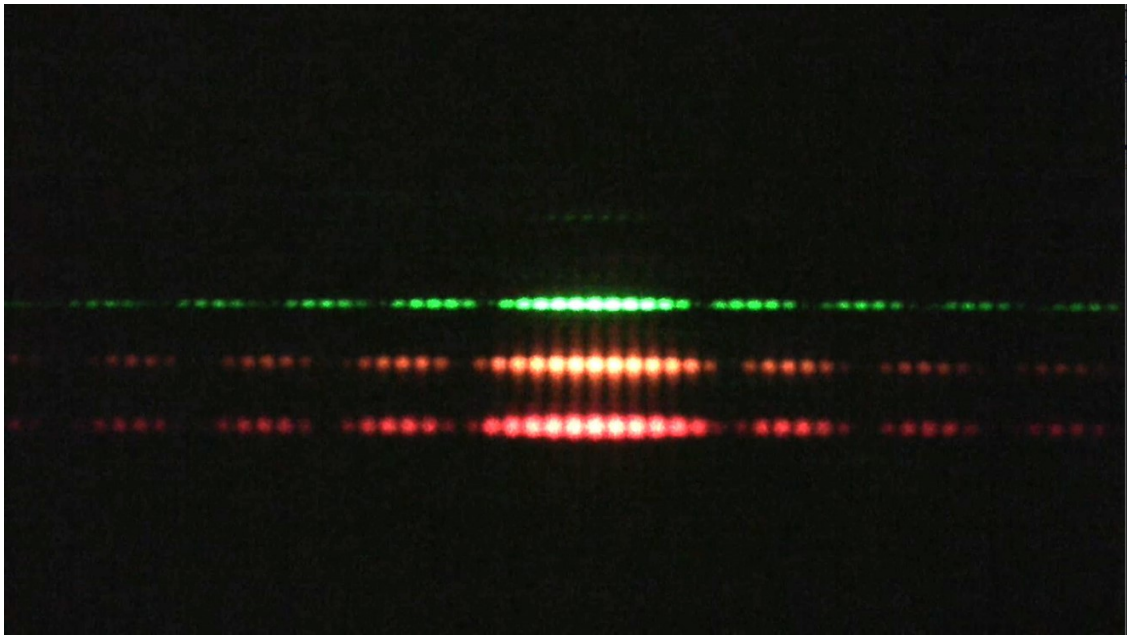

Therefore, the distance between absorption fringes is inversely proportional to the momentum of the photons used in the experiments.

As we have seen in this section, the emergence of fringe patterns in double-slit experiments can be explained in terms of absorption and reflection of photons using the singularly corpuscular model of light proposed by QGD. In fact QGD's corpuscular model and the laws of momentum together explain all optical phenomena which are normally attributed to wave-like behaviour of light. In fact, all optical phenomena can be described a single consistent set of equations that can replace the distinct equations currently used to describe distinct phenomena.

QGD Explanation of Quantum Entanglement Experiments

Preonics provides simple and realistic explanations of observations of so-called quantum entanglement experiments. Not only is QGD consistent with the experimental observations of so-called quantum entanglement experiments but, unlike quantum mechanics, precisely explains the mechanisms responsible for outcomes currently attributed to quantum entanglement effect without violating the principle of locality. The simple experiment below is an example of how to preonics can be used to analyse of an experiment and predict its outcome.

In the setup shown in figure 1, which is called a Mach-Zehnder Interferometer, we have a source of light which beam is split in two by a half-silvered mirror. The classical prediction is that 50% of the light will be reflected to the mirror on the top left (path 1) and 50% will be refracted to the mirror at the bottom right (path 2). The light which arrives at the top left mirror will be reflected towards the back side of the half-silver mirror on the top right where it will be split into two beams towards detector 1 and detector 2, each of which should be receiving 50% of the photons coming through path 1 or with 25% of photons emitted by the source.

figure 1

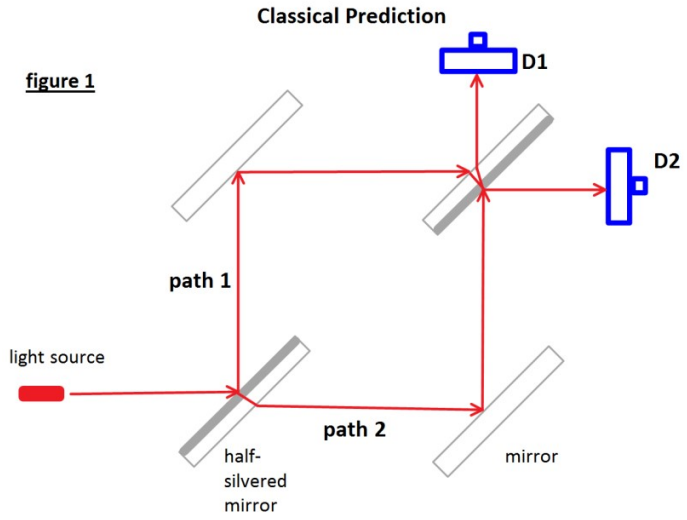

The photons that follows path 2 (50% of the photons from the source) is reflected by the mirror at the bottom right towards the half-silvered mirror at the top right where it will be split into two beams each having 50% of the photons following path 2 (or 25% of the photons from the source beam). So classical optics predicts that 50% of the photons from the source will reach D1 and the other 50% will each D2. However observations show that 100% of the photons from the source reach D2 and none reach D1 (figure 2).

figure 2

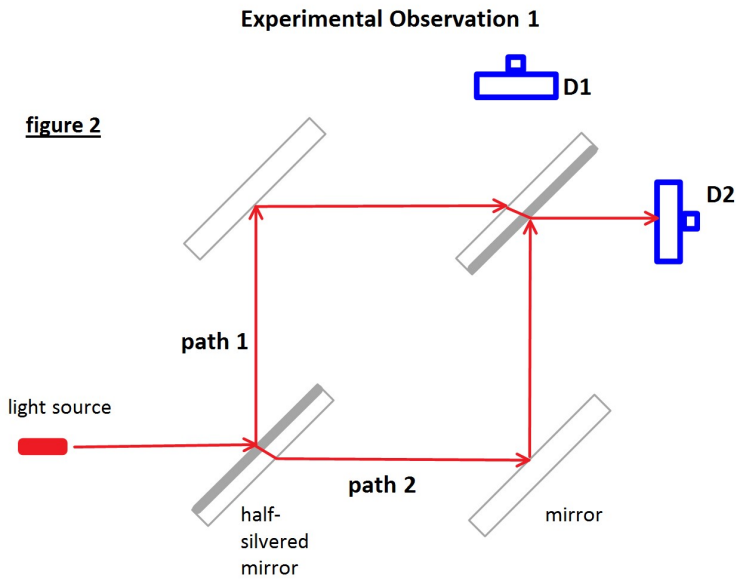

The explanation provided by quantum mechanics, which is similar to that given for the results of double-slit experiments, proposes that the wave function of each individual photon travels both paths and engages in interference at the half-silvered mirror on the top right and that they interfere destructively at D1 and constructively at D2 (a detailed explanation can be found here).

Applying the QGD optics to analyse the setup, we find a different and much simpler explanation.

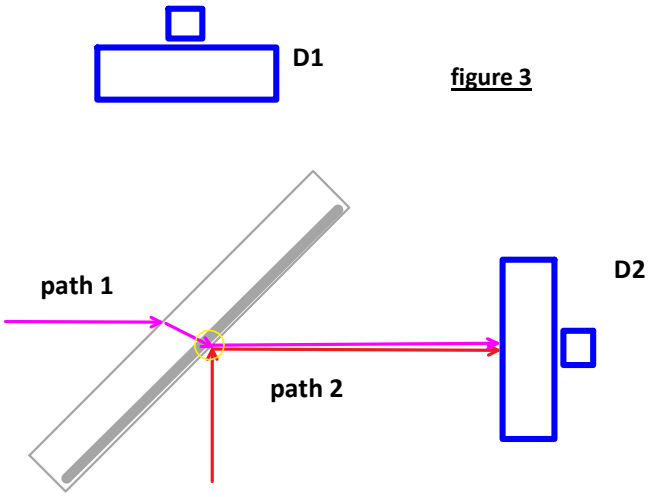

figure 3

At the point of intersection in the top right half-silvered mirror (yellow circle in Figure 3), $\left\| \vec{P}_{\gamma_1} \cos_{\theta_1} + \vec{P}_{\gamma_2} \cos_{\theta_2} \right\| < m_{e^-}$ so that the photons γ_2 are reflected to D2 as per the mechanism of reflection we described above.

Now consider the setup shown in figure 5. Observations show that in this setup 50% of the photons reach D3, 25% of the photons that will reach each of D1 and D2 detectors.

Experimental Observation 2

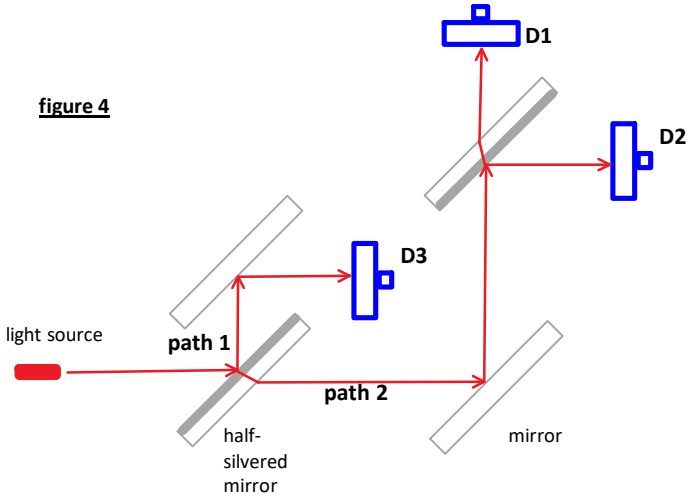

figure 4

According to quantum mechanics, the photons moving along path 2 that reach D1 can only do so if the photons moving along path 1 are deflected towards D3. This raises the question: How the photons that reach D1 know that the photons of path 1 were deflected towards D3?

The quantum mechanical explanation is that the photons from path 1 and path 2 are entangled, a phenomenon known as quantum entanglement, by which a change done to photons on path 1, by a measurement for example, instantly affects the photons moving on path 2. And, according to quantum mechanics, it does so instantly and independently of the distance that separate the entangled photons. This explanation of course violates locality, but this violation is essential to quantum mechanics if it is to describe the observations of experiments such as the ones we described above. The observations in turn, *as interpreted by quantum mechanics*, support the existence of quantum entanglement and non-locality.

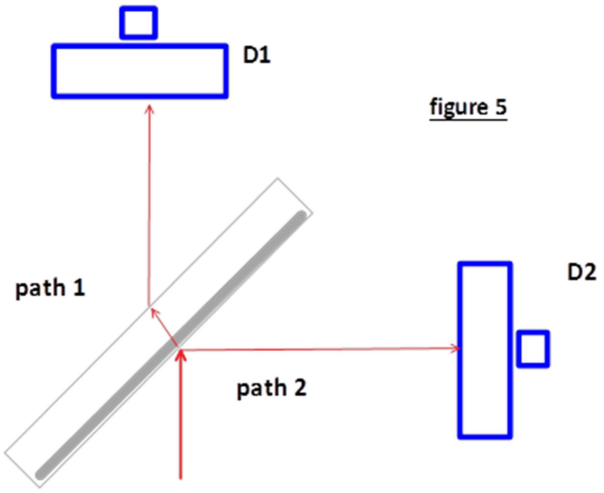

figure 5

Again QGD provides a much simpler and realistic interpretation of observations. That is: Since no photons from path 1 reach the point of interaction of top right mirror, then then $\vec{P}_{\gamma_1}\cos_{\theta_1}=0$ and $\left\|\vec{P}_{\gamma_1}\cos_{\theta_1}+\vec{P}_{\gamma_2}\cos_{\theta_2}\right\|>m_{e^-}$. That the mirror is transparent to photons of momenta $\left\|\vec{P}_{\gamma_2}\right\|$, means that $\left\|\vec{P}_{\gamma_2}\right\|\gg m_{e^-}$ so the photons γ_2 from path 2 can be absorbed by the outer electrons and allowed to move towards D1 as per the refraction mechanism we described earlier.

The example above illustrates that the outcome of so-called quantum entanglement can easily be explained classically from a complete physical description of the experiments. Complete physical descriptions of all other experiments supporting quantum entanglement will also provide the basis for classical explanations.

QGD interpretation of the redshift effect

Quantum-geometry dynamics tells us that the energy of a photon is given by $E_\gamma = \sum_{i=1}^{m_\gamma} \left\| \vec{c}_i \right\| = m_\gamma c$ were $\vec{c}_i$ is the momentum vector of a component $preon^{(+)}$. The energy of a photon is proportional to its mass.

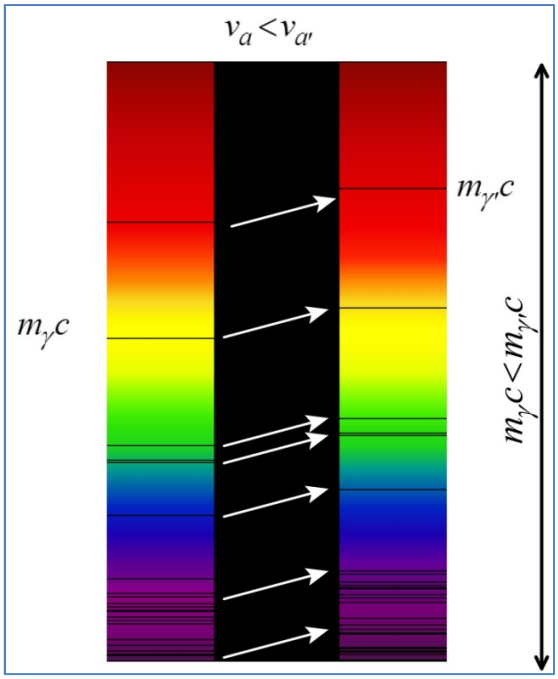

Applying the laws of transfer of momentum for a photon γ to a particle, structure or other target a, we find that the momentum transferred is $\left\| \Delta \vec{P}_a \right\| = \left(c - v_a \right) m_\lambda$ where v_a is the intrinsic speed of a relative to γ . For a second photon γ' coming different direction but where $m_{\gamma'} = m_\gamma$ but $\vec{P}_{\gamma'} \neq \vec{P}_\gamma$, then $\left(c - v'_a \right) m_\gamma \neq \left(c - v_a \right) m_\gamma$ and the different in the momentum imparted is given by $\left(v_a - v'_a \right) m_\gamma$. That is: $\left\| \Delta \vec{P}_{a_{\gamma'}} \right\| < \left\| \Delta \vec{P}_{a_\gamma} \right\|$.

If the light from a is used as a reference then if $v_a < v_{a'}$ then we would observe a redshift of the absorption band. If $v_a > v_{a'}$ then we would observe an blueshift of the absorption band (figure on the right).

Therefore, we have shown that QGD explains the observations of shift in absorption bands (and emission bands since allowable changes in momentum obey the same laws) and does so using a model of light that is singularly corpuscular. Unlike the wave-particle model, QGD's mechanisms of the redshift and blueshift effect conserve energy since $\sum_{i=1}^{m_a} \left\| \vec{c}_i \right\| + \sum_{j=1}^{m_\gamma} \left\| \vec{c}_j \right\| = \sum_{i=1}^{m_a + m_\gamma} \left\| \vec{c}_i \right\|$.

It is important here to keep in mind that the speed v_a and $v_{a'}$ are the intrinsic speed of the atomic electrons from the sources and not the speed of the sources themselves. If to a given quantum state of an atomic electron corresponds a specific momentum, then the shift must be due difference in the speed of the sources themselves. That is $v_a = v_{e^-} + v_x$ and $v_{a'} = v_{e^-} + v_{x'}$ where x and x' are the astrophysical bodies emitting the light so that $\left(c - \left(v_{e^-} + v_x \right) \right) m_\gamma = \left(c - \left(v_{e^-} + v_{x'} \right) \right) m_{\gamma'}$.

QGD's description is consistent with the observation of the redshift and blueshift, yet there are important distinctions. For instance, since the energy of a photon is intrinsic, it is independent of the frame of reference in which it is emitted, travels or absorbed.

Also, the laws and mechanisms used to describe and explain the redshift effect also explain all other optical effects, even the observed fringe patterns in double-slit experiments and that without the wave-particle duality concept.

The Measurement of Physical Properties and Frames of Reference

According to QGD:

- m_a, the mass of an object a, is equal to the number of $preons^{(+)}$ that compose it;
- E_a , its energy, is equal to its mass multiplied by the fundamental momentum of the $preon^{(+)}$; that is: where $\vec{c}_i$ is the momentum vector of a $preon^{(+)}$ and $c = \|\vec{c}_i\|$ is the fundamental momentum, then $E_a = \sum_{i=1}^{m_a} \|\vec{c}_i\| = m_a c$.
- $\vec{P}_a$, the momentum vector of an object, is equal to the vector sum of all the momentum vectors of its component $preons^{(+)}$ or $\vec{P}_a = \sum_{i=1}^{m_a} \vec{c}_i$ and P_a , its momentum, is the magnitude of its momentum vector. That is: $P_a = \|\vec{P}_a\| = \left\| \sum_{i=1}^{m_a} \vec{c}_i \right\|$ and finally
- v_a , its speed, is the ratio of its momentum over its mass or $v_a = \frac{P_a}{m_a} = \frac{\left\| \sum_{i=1}^{m_a} \vec{c}_i \right\|}{m_a}$.

All the properties above are intrinsic which implies that they are qualitatively and quantitatively independent of the frame of reference against which they are measured. We must however make the essential distinction between the measurement of a property of an object and its actual intrinsic property.

Take for instance the speed of light which we have derived from the fundamental description of the properties of mass and momentum and shown to be constant. That is: $v_\gamma = \frac{P_\gamma}{m_\gamma}$ and since, for momentum vectors of photons all point in the same direction we have $P_\gamma = E_\gamma$ and $v_\gamma = \frac{P_\gamma}{m_\gamma} = \frac{E_\gamma}{m_\gamma} = \frac{m_\gamma c}{m_\gamma} = c$.

If we were to experimentally measure the speed of light, or more precisely, the speed of photons, we would set up instruments within an agreed upon frame of reference. We would

map the space in which the measurement apparatus is set and though the property of speed is intrinsic, thus independent of the frame of reference, the measurement of the property is dependent on the frame of reference. But if, as we know, the speed of light has been observed to be independent of the frame of reference, then how can this be reconciled with QGD's intrinsic speed?

Before moving forward with the experiment it is important to consider what it is that our apparatus actually measures. Speed is conventionally defined as the ratio of displacement over time, that is $v = \frac{d}{t}$ where d the distance is and t is time. Space and time here are considered physical dimensions and as a consequence the conventional definition of speed is never questioned.

Distance can be measured by something as primitive as a yard stick and its physicality is hard to argue with. Time and its physicality pose serious problems. Time is assumed to be measurable using a clock of some sort but, it is easily shown that clocks are simply cyclic and periodic systems linked to counting devices and they do not measured time but merely count the number of repetitions of arbitrarily chosen states of these systems.

So conventional speed in general, and that of light in particular, is simply the distance in conventional units something travels divided by the number of cycles a clock goes through during its travel. Therefore the conventional definition of speed, which is the ratio of the distance travelled by an object over the number of cycles, is not the objects speed, but of the distance travelled between two cycles. That goes for the speed of photons.

There is a relation between conventional speed and intrinsic speed and we find that the conventional speed of a photon is proportional to its intrinsic speed, that is $\frac{d}{t} \propto v_\gamma$, but while conventional speed is relational (and not physical since time itself is not physical) , the intrinsic speed is physical since it is derived from momentum and mass, both of which are measurable, hence physical.

Now going back to frames of reference, let us assume a room moving at an intrinsic speed v_a . A source of photons is placed at the very centre of the room which photons are detected by detectors placed on the walls, floor and ceiling. The source and detectors are linked are in turn linked to a clock by wires of the same length. The clock registers the emission and the reception of the photons in such a way that we can calculate the conventional speed of photons. For now, we will assume that the direction of motion of the room is along the x axis.

QGD predicts that even though the intrinsic speed of photons is reference frame independent, their one way conventional speed to detector D_{x_1} will be larger than their one way conventional

speed at the detector D_{x_2}. The relativity theory predicts that the conventional speed of photons will be the same at both detectors independently of v_a. So all that is needed to test which theory gives the correct prediction is to make one way measurements of the conventional speed of photons. Problem is; all measurements of the speed of light are two way measurements and since any possible contribution of v_a to the conventional speed of photons traveling in one direction is cancelled out when it is reflected in the other direction. In other words since both QGD and the relativity theory predicts the two way measurements will be equal at D_{x_1} and D_{x_2} such experiments cannot distinguish between QGD and the relativity theory.

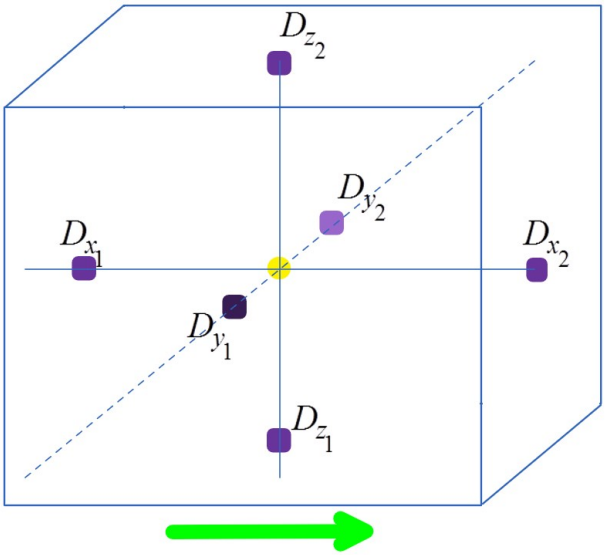

However, a similar experiment which measures not speed but momentum can distinguish between the theories. The photons at detector D_{x_2} will be redshifted while those at D_{x_1} would be blueshifted. Both theories predict $P_{D_{x_1}} > P_{D_{x_2}}$ but their predictions for the other detectors are different.

Assuming that the room's motion is align with the x axis[10], the relativity theory predicts that $P_{D_{x_1}} > P_{D_{y_1}} = P_{D_{y_2}} = P_{D_{z_1}} = P_{D_{z_2}} > P_{D_{x_2}}$. For the same experiment the QGD theory predicts $P_{D_{x_1}} = P_{D_{y_1}} = P_{D_{y_2}} = P_{D_{z_1}} = P_{D_{z_2}} > P_{D_{x_2}}$.

If QGD's prediction is verified, then the intrinsic of the frame of reference can be calculated using the equations we introduced earlier to describe the redshift effect. That is; from our description of the redshift effect, we know that $P_\gamma = \Delta P_{D_{x_1}}$ then we have $\frac{c - v_a}{c} m_\gamma = P_\gamma - \frac{v_a}{c} = P_{D_{x_1}} - \frac{v_a}{c} = P_{D_{x_2}}$ and $v_a = \left(P_{D_{x_1}} - P_{D_{x_2}}\right)c$.

Once the intrinsic speed of a reference system is known, then it can be taken into account when estimating the physical properties of light emitting objects from within it.

[10] The alignment with the x axis is found by rotating that detector assembly so that the D_{x_2} detector measures the lowest momentum (largest redshift).

QGD's description of the redshift effect implies distinct predictions for all observations based on redshifts measurement but I would like to bring attention to one direct consequence which has been confirmed by observations; the observed orbital speed of stars around their galactic centers .

Quantum-Geometrical Space and Coordinate Systems

The nature of quantum-geometrical space allows us to have a direct correspondence between every individual $preon^{(+)}$ that forms it and the points of reference systems. We can arbitrarily choose a system of axis and their origin, but such choice does not in any way affect the measurements of physical properties or position of an object in quantum-geometrical space. All such reference systems are equivalent only requires the necessary changes in coordinates. So not only are the determination of physical properties from measurements independent of the frame of reference used, but also is their positions.

The Measurement of the Rotation of Galaxies and Redshifts

We have shown that the redshift effect is dependent on the speed of the detector relative to the intrinsic speed of the photon. This provides a very different interpretation of the redshift observations from distant galaxies. The usual theoretical interpretation of the redshift, as dependent on the motion of the source relative to the detector is used to measure the speed of distant objects, including the rotation speed of galaxies.

The classical interpretation of the redshift gives speeds of rotation that are not in agreement our best theories of gravity which predicts the nearer star are to its galactic center, the greater their speeds should be. But that is not what was observed.

The orbital speeds of stars, estimated from their redshifts, are about the same regardless of their distance from their galactic centre. This led to the introduction of dark matter models to explain the discrepancy between predictions and observations. QGD does not dispute the existence of dark matter which existence it predicts and is supported by a number of observations that do not depend on redshifts measurements. However, QGD shows that the redshifts from all stars from a galaxy will be the same independently of their speed. In other words, even if their actual orbital speeds are in agreement with our theories of gravity, their redshifts will be the same. Hence the orbital speeds of stars derived from the accepted redshift interpretation will give similar speeds in agreement with observations.

Prediction

QGD predicts that the angular and axial speeds of stars estimated through their parallax will show them to be dependent on their distance from the galactic center. GAIA , which is underway, will be making such observations which could confirm QGD's prediction.

Distances and Intrinsic Luminosities of 1a Supernovas

First we need to choose a reference type 1a supernova with the largest blueshift and measure its distance d_{ref} from it parallaxes so as to eliminate physical assumptions (such measurement will be possible using the data from the GAIA or similar mission). Based on QGD's explanation of the redshift effect, we understand that the electromagnetic emission from such a supernova is its intrinsic spectrum.

Once the distance is known, we can calculate its intrinsic luminosity using the formula $L_{ref} = Flux_{\gamma_{ref}} * 4\pi d^2$ where the $Flux_{\gamma_{ref}}$ is the number of photons γ_{ref} of a given momentum or energy (since these properties are numerically equal for photons).

In order to measure the distance of another type 1a supernova (*SN*) we must determine its redshift. The redshift is used here to determine the position on the redshifted spectrum of the supernova where we will find photons γ_{SN} that have the same intrinsic energy as the reference photons γ_{ref}. $Flux_{\gamma_{SN}}$ is the number of γ_{SN} photons.

If the luminosities of type 1a supernovas are comparable (the accepted assumption), that is: if $L_{ref} = L_{SN}$, then $L_{ref} = Flux_{\gamma_{SN}} * 4\pi d_{SN}^2$ and $d_{SN} = \sqrt{\frac{L_{ref}}{4\pi Flux_{\gamma_{SN}}}}$.

Derivation of the Intrinsic Speed of Earth from Type 1a Supernovas

Also, using QGD's description of the redshift effect, we can calculate $\vec{v}_a$, the intrinsic speed of the Earth (or that of any detector in space), using three non-coplanar reference supernovas.

Since $\left(\vec{c}_{\gamma_{SN_i}} - \vec{v}_{a_{SN_i}}\right) m_{\gamma_{SN_i}} = \Delta\vec{P}_a$, then $\vec{v}_{a_{SN_i}} = \vec{c}_{\gamma_{SN_i}} - \frac{\Delta\vec{P}_a}{m_{\gamma_{SN_i}}}$ and

$\vec{v}_a = \vec{v}_{a_{SN_1}} + \vec{v}_{a_{SN_2}} + \vec{v}_{a_{SN_3}}$.

Conclusion

If QGD's explanation of the redshift effect is confirmed, then it will be possible to measure the intrinsic speed not only of the Earth (its absolute speed) but of other observable objects and from it, derive the values of other intrinsic properties such as momentum and mass.